ACS OMEGA

http://pubs.acs.org/journal/acsodf

Article

Development of a Microfluidic Method to Study Enhanced Oil Recovery by Low Salinity Water Flooding

Marzieh Saadat, Peichun A. Tsai,* Tsai-Hsing Ho, Gisle Øye,* and Marcin Dudek

Cite This: *ACS Omega* 2020, 5, 17521−17530

Read Online

ACCESS | Metrics & More | Article Recommendations

ABSTRACT: Microfluidics is an appealing method to study processes at rock pore scale such as oil recovery because of the similar size range. It also offers several advantages over the conventional core flooding methodology, for example, easy cleaning and reuse of the same porous network chips or the option to visually track the process. In this study, the effects of injection rate, flood volume, micromodel structure, initial brine saturation, aging, oil type, brine concentration, and composition are systematically investigated. The recovery process is evaluated based on a series of images taken during the experiment. The remaining crude oil saturation reaches a steady state after injection of a few pore volumes of the brine flood. The higher the injection rate, the higher the emulsification and agitation, leading to unstable displacement. Low salinity brine recovered more oil than the high salinity brine. Aging, initial brine saturation, and the presence of divalent ions in the flood led to a decrease in the oil recovery. Most of the tests in this study showed viscous fingering. The analysis of the experimental parameters allowed to develop a reliable and repeatable procedure for microfluidic water flooding. With the method in place, the enhanced oil recovery test developed based on different variables showed an increase of up to 2% of the original oil in place at the tertiary stage.

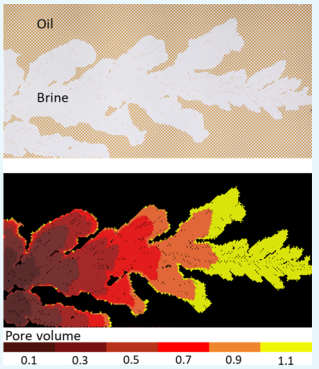

1. INTRODUCTION

Currently, more than half of the original oil in place is left behind in the reservoirs after shutdown.[1,2] At this scale, even slight improvements in extraction would result in an enormous amount of additional recovered oil and value for the society while reducing the environmental impact. Enhanced oil recovery (EOR) methods are techniques that are employed after the natural drives (such as fluid expansion and rock compressibility) and injection of seawater or gas (to support the pressure) fail to produce more oil. Much of the oil remaining in the reservoir prior to this stage is microscopically trapped in the pores by capillary action. The amount of remaining oil depends largely on the ratio between the viscous forces displacing the oil and the capillary forces trapping the oil. The interactions between crude oil, brine, and reservoir rocks are essential for the efficiency of recovery. This means that how much, how fast, and how completely oil can be extracted from a reservoir is primarily governed by phenomena and processes that occur at the pore level, that is, length scales in the micrometer range.

Water flooding is the most widespread method in both secondary and tertiary oil recovery modes. Utilizing low salinity (LS) brine as an EOR method has gained much attention by researchers since Tang and Morrow[3] introduced the idea in 1997. Literature has shown that LS EOR is an effective method that decreases the residual oil saturation. Based on core flooding experiments and field trials, it has shown to increase oil recovery by 2−40% in both carbonate and sandstone rocks.[4−6] The efficiency of the brine also depends on the composition and ionic strength.[7,8] For example, crude oil−water interfacial tension (IFT), as one of the effective factors in oil recovery, can vary by three orders of magnitude as a function of calcium to sodium ratio.[9] Despite the large number of recent studies in this area, a consistent mechanism has not been concluded.[7,10] Suggested mechanisms include fine migration,[11,12] local increase in pH at the clay surface,[13,14] multicomponent ionic exchange,[4] destabilizing oil−rock adhesion,[15] and osmosis[16] among others. A larger number of studies agree that wettability alteration is the mechanism for LS water flooding oil recovery.[17−20]

The classical way of studying EOR is by core flooding investigations, which can give useful information about both the kinetics and the amount of oil recovered. A limitation, however, is that manipulation of the fluids and direct observations of underlying mechanisms and critical phenomena at the pore level are not possible, and only the overall behavior of the systems can be described. Furthermore, core flooding is time-consuming, and the reproducibility of the experiments is an inherent challenge.

A powerful method of investigating oil displacement is the real-time direct observation of the phenomena through the porous media. This was challenging to achieve prior to

Received: April 30, 2020
Accepted: June 26, 2020
Published: July 10, 2020

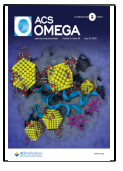

microfluidics. A microfluidic system, here reservoir-on-a-chip, is a device where microvolumes of fluids can be controlled and studied in microchannels or networks of microchannels, and the fluid behavior is often recorded via microscopy. Such a technique is well-suited for visualization and fundamental studies of the phenomena governing oil mobilization and displacement at length scales where capillary forces dominate.[21−23] With microfluidics, one can simulate pore networks in oil reservoirs and provide high-resolution data for a better understanding of liquid front propagation and fluid displacement to increase sweep efficiency and minimize undesired effects such as viscous fingering.

Some efforts have been made to conduct fundamental studies or to mimic EOR processes using microfluidics. This includes studies where systematic variations of the capillary number (Ca) and the viscosity ratio (M) between the displacing and displaced fluids were used to determine transitions from unstable displacement by viscous or capillary fingering to stable displacement.[24−26] Lenormand and co-authors[25] also ran computer simulations on different networks over a range of capillary numbers (Ca) and viscosity ratios (M). They consequently produced a phase diagram of Ca versus M to show where each displacement mechanism is dominant. It was suggested that the result also depends on pore geometry and topology.

Crude oils are complex fluids that contain interfacially active fractions such as resins and asphaltenes. These fractions will undergo adsorption/desorption processes at the pore surfaces at various conditions. When crude oil fills a pore system, asphaltenes and resins will adsorb onto the pore walls and likely make the surface less hydrophilic. Upon displacement of the crude oil by aqueous EOR fluids, asphaltenes and resins can desorb from the pore walls and make the surface more water-wet. The extent of adsorption, desorption, and wettability alteration would depend on both the crude oil properties and the type of EOR fluid.[27,28] Notably, in displacement studies using model oils, these phenomena are not an issue.

Recent microfluidic investigations have utilized various pore networks in the displacement studies, while one study has investigated mobilization of oil in a single-pore scale.[29] Some studies have used crude oil to visualize multiphase flow,[30−32] while others have used model oils.[2,33] A missing link in microfluidic studies is that most studies only look at one variable. While this provides valuable in-depth knowledge of the matter, the results cannot be projected to other systems. In other words, microfluidic studies investigate different factors but vary in setup, materials, conditions, and procedures. Although they may cover many variables altogether, hardly any two studies share the same base for comparison.

In developing a practical methodology for studying oil recovery, the effect of many key parameters must be considered. The goal for this study is to assess the variables and develop a reliable experimental procedure. Experiments were designed and performed accounting for parameters including flood flow rate, flood volume, oil type, initial brine saturation (wetting the chip with brine before oil saturation), network design, brine concentration, and brine composition. Crude oil samples were used to fill the gap in microfluidic literature and gain better knowledge about how the physicochemical properties of the oil and water phases and the pore properties are linked. Moreover, this study, as part of a bigger project, provides the opportunity to assess the exact same system and procedure with varying reservoir conditions and flood types to provide comprehensive understanding and strategy for better oil recovery.

2. MATERIALS AND METHODS

2.1. Porous Media. We used two types of micromodels from Micronit Microtechnologies (uniform and rock network) to investigate the effect of the pore structure. The chips are made of borosilicate glass through isotropic etching and are hydrophilic. They consist of inlet and outlet channels, which are designed for even introduction and distribution of the fluid to the network, as well as a network of throats and pores, which is the area of interest in the analysis. Because the size scale of the pores is comparable to that of the reservoirs, it is a well-suited representation of the in situ structure for the two-phase immiscible displacement experiments. The micromodels would ideally mimic sandstone rocks because of their inherent wettability resulting from surface silanol groups. The limitation, however, would be not accounting for clays.

In uniform network pore models, channels represent throats and intersection model pores. This constitutes the simplest version of an interconnected pore network and is used to investigate the displacement of the crude oils by aqueous EOR fluids. The throats are 50 μm wide, and pores are 90 μm in diameter. The etched depth is 20 μm. Figure 1 (left) depicts the

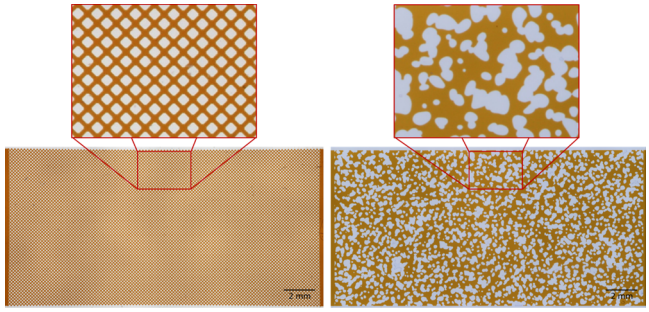

Figure 1. Illustration of the two pore models (filled with crude oil): uniform network (left) and rock network (right). The scale bar is 2 mm.

structure of the uniform-network micromodel. For a better representation of a rock, another type of micromodel was also used in this study. Random placement of morphologically different pores and throats based on the cross-section profile of a carbonate rock makes up the rock network micromodel (Figure 1 right). The porosity of the uniform network and rock network chips is 0.52 and 0.57, respectively.

2.2. Crude Oils. Three crude oils with different chemical composition from the Norwegian Continental Shelf were used in this study. Crude oils are used as the displaced phase inside the micromodels. Crude oil F is dyed with Sudan III (Sigma-Aldrich) for better contrast to the water phase. Table 1 provides information on the properties of the crude oils.

2.3. Brines. Four different brine solutions were prepared using deionized water, NaCl, and $CaCl_2$. A pair of LS brine with 0.02 M ionic strength was made, one of which contained only NaCl (LS-Na), and the other included both monovalent and divalent ions, sodium and calcium (LS-NaCa). The ionic strength is about the same value reported in other studies.[35,36] The other pair was high salinity (HS) brines of 0.6 M ionic strength, with and without $CaCl_2$ (HS-NaCa and HS-Na). The calcium-to-sodium molar ratio for the LS water was selected to be 0.02 based on the optimum ratio reported in a previous study.[35] The same ratio was also used for the HS water. The HS

https://dx.doi.org/10.1021/acsomega.0c02005
ACS Omega 2020, 5, 17521−17530

Table 1. Physicochemical Properties and Compositions of Crude Oils.[34]

	API [deg]	viscosity [mPa·s] @ 20 °C	TAN [mg KOH/g oil]	TBN [mg KOH/g oil]	SARA [% wt]			
					saturates	aromatics	resins	asphaltenes
crude oil A	19.2	354.4	2.2	2.8	50.6	31.2	15.7	2.5
crude oil C	23	74.4	2.7	1.1	64.9	26.3	8.4	0.4
crude oil F	39.7	7.5	0.1	0.6	78.5	18.9	2.5	0.1

brine represents seawater, abundantly available for pressure support at the secondary stage at the Norwegian Continental Shelf and matches the ionic strength reported in the literature.[13,37] They were used as the displacing fluid in the micromodels. The properties of the brines are provided in Table 2.

Table 2. Displacing Fluid Properties

flood name	symbol	ionic strength (M)	Ca/Na (mole/mole)	viscosity (mPa·s)
HS brine	HS-Na	0.6	0	1.14
HS brine	HS-NaCa	0.6	1/50	1.09
LS brine	LS-Na	0.02	0	1.06
LS brine	LS-NaCa	0.02	1/50	1.03

The IFT between the crude oils and different aqueous floods were measured by a SVT20 spinning drop tensiometer (DataPhysics Instruments, Germany). The IFT values are recorded after the measurements were stable for 20 min.

2.4. Experimental Setup. The experimental setup consists of a syringe pump, imaging setup, pressure sensor, and microfluidic device. Two separate but similar setups at the University of Alberta and Norwegian University of Science and Technology were used for conducting the experiments in this study. The syringe pump is Chemyx Fusion 4000 and is used for flooding the chips with accurate and specifically low flow rates during the experiments. It is also used to inject the solvents during the cleaning procedure. The micromodel is placed in a chip holder that provides an interface to connect the chip to inlet and outlet tubing so that the fluids can be injected into and produced from the pore models. High-resolution cameras (Canon EOS 70D and 90D) and macrolenses were used. The cameras were connected to and controlled by a computer. A flat light-emitting diode backlight was used to illuminate the micromodels. The pressure sensors by LabSmith and ElveFlow were used to record the pressure during flooding. They measure up to 1800 kPa and 100 psi, respectively. The accuracy for the LabSmith pressure sensor is 1% of the full scale. This number is 0.2% of the full scale for ElveFlow. The setup is schematically illustrated in Figure 2.

2.5. Procedure. To evaluate one variable, all other parameters were fixed between two tests. Therefore, the procedures and test conditions vary for each experiment. However, the general procedure is as follows:

If the test involves initial brine saturation, the chip is initially filled with HS brine before the oil-saturating step. Otherwise, the empty clean micromodels are filled with crude oil. Oil saturation is followed by a short adsorption time that likely affects the wetting conditions. Then, the flood fluid gets injected using the syringe pump. The injection rate in this study is fixed at 0.5 μL/min for all experiments, except the tests that are studying the effect of the flow rate. In that case, the injection rate varies between 0.03 and 50 μL/min. Depending on the experiment, the flood can be any of the four (high or LS) brines (Table 2). All

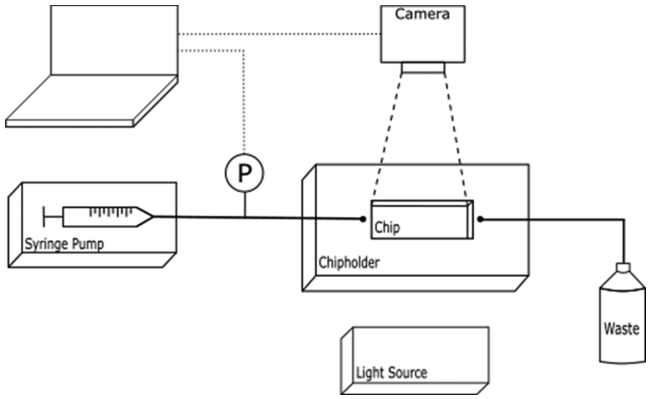

Figure 2. Schematic illustration of the microfluidic setup. The setup is operated at room temperature (22 °C). Dimensions shown are not to scale.

steps were performed at room temperature (22 °C). The course of each displacement process is visually accessible, and snapshots are captured using an overhead camera. The dynamic pressure of the tests is also recorded. Each test was carried out three times. The values reported are the average of the three with the standard deviation as the error bar.

ImageJ is utilized to analyze the images. Images are processed by color thresholding based on saturation and brightness before they are converted to 8-bit pictures. Then, the oil saturation is evaluated for each image based on the ratio of the colored area (remaining oil in the network) to the whole area of interest (fully saturated network) based on the number of pixels. By using a calibration ruler, the numbers in pixels can also be translated to μm values. The recovery factor (RF) is then calculated as the ratio of extracted oil to the original oil in place

$$\mathrm{RF}=\frac{S_i - S_f}{S_i}$$

where S_i and S_f are the initial and final saturation of oil in the network, respectively. Because tens of pictures are typically taken for each measurement, the evolution of the RF as a function of time or pore-volume injected can also be presented.

The chips are reused in this study. Therefore, they go through a thorough cleaning procedure after each test. It includes flooding the chip first with xylene, then isopropanol, deionized water, and air. The solvents, xylene, isopropanol, and water are used to make sure any participant in the tests is dissolved and removed from the chips. In the end, the chips are baked at 475 °C in a furnace to dry, or to disintegrate any residuals, and ensure the cleanliness of the chips for the next tests.

2.6. Aging Setup. Aging the oil inside the network is an important step of oil recovery tests. However, it proved to be challenging as, with time, the oil evaporates from the openings of the network. This would introduce a third phase, that is, air bubbles into what would otherwise be an oil−water system. In order to age the chips without losing oil, an aging setup was designed to plug the inlet and outlet of the chips. The setup is

https://dx.doi.org/10.1021/acsomega.0c02005
ACS Omega 2020, 5, 17521−17530

designed to hold multiple chips at the same time and was built at the mechanical workshop of the Faculty of Natural Sciences, NTNU. Plugs are used to block the micromodel inlets and outlets to prevent evaporation.

3. RESULTS AND DISCUSSION

3.1. Pressure Data. Tracking the pressure was specifically useful at the experiment development stage. It helped troubleshoot and make sure there are no leaks or blockages on the line or inside the chip. In this way, we could assure a reliable and repeatable experiment.

The typical trend for the pressure is as follows: the pressure increases almost steadily since the syringe pump starts pumping and as the flood goes through the network. The maximum pressure is reached right before the breakthrough, that is, when the flood gets to the end of the network. After the breakthrough, if the oil content of the micromodel is not changing, the pressure drops sharply close to ambient pressure. However, in cases where there are multiple breakthroughs or oil extraction continues after the first breakthrough, the pressure has a more subtle and gradual decline to ambient pressure. Figure 3

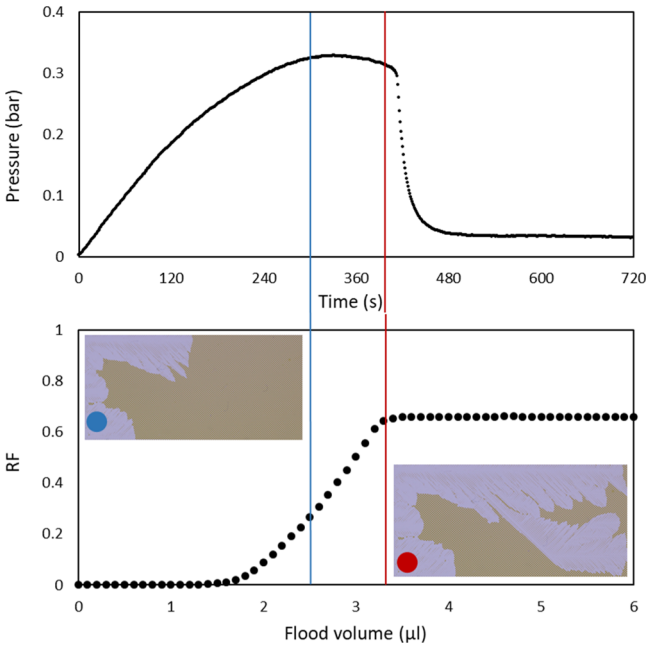

Figure 3. Changes of pressure and RF with time for crude oil A displaced by HS-NaCa at 0.5 μL/min.

demonstrates a typical pressure graph along with the corresponding RF graph. The two graphs are vertically matched so that the corresponding changes between RF and pressure can be tracked. The blue line and its image mark a point before the breakthrough happens, and the red one shows precisely when the breakthrough happened. The sudden pressure drop happens shortly after that. It takes about 10 s for the pressure to reflect the breakthrough as the water gets through the outlet channel.

The maximum pressure increases with the increasing flood flow rate. Among different oils, the lighter oils show lower pressures. It is expected to record a higher pressure for a rock network rather than a uniform network because of irregular morphology of the pores and, more importantly, the dead-end pores and narrow throats. This was also confirmed by the experiments, and higher pressure was recorded for the rock network. Brine concentration does not seem to influence the pressure, while the presence of the divalent ion in the flood increased the recorded pressure. This could be explained by the stronger bonds that the divalent ions create between the negatively charged surface and the negatively charged acidic groups of the oil. The higher viscosity of crude oil and higher flood injection rate also cause the higher pressure.

3.2. Oil Type. The three crude oils, with a rather broad range of properties, were flooded with HS-Na. Figure 4 shows the course of the recovery process for the oils until the breakthrough. Immiscible fluid−fluid displacement in a porous media can be either stable or unstable. Stable displacement is when the flood forms an almost straight and compact oil−water frontline while displacing the oil. The frontline propagates to sweep the whole network until it gets to the outlet. Because all tests in the current study have a lower viscosity fluid displacing a more viscous one, stable displacement only happened for the lightest oil, crude oil F. Crude oil F goes through a stable displacement and recovers 93% of the original oil in place. Any other type of displacement is categorized as unstable. Unstable displacements in this study happened in different patterns depending on the test conditions. They vary in how and to what extend the flood spreads out through the network area. Figure 4 also shows the process of displacing crude oil C with HS-Na. It starts as a couple of wide streams that either eventually join or, in combination, would cover almost the whole network area of the chip. In this case, we observed two breakthroughs. Finally, Figure 4 demonstrates the displacement of crude oil A by HS-Na. The figure also shows that the breakthrough time, or the pore volumes injected until breakthrough, also depends on the oil type and the pattern. Generally, it takes longer for the stable displacement to reach breakthrough because of larger covered area and higher sweep efficiency. In case of unstable displacements, multiple breakthroughs and larger flooded area result in longer recovery times.

The RFs along with images of the remaining oil in channels after the flood are summarized in Figure 5. The RFs for different oils are different. Based on the graph, crude oil F has the highest, while crude oil A has the lowest recovery efficiency. The lower the viscosity of the crude oil, the higher is the RF. Moreover, crude oil F has the lowest resin and asphaltene fraction and acid number. This means the oil is expected to have the least amount of interfacially active and polar components, thereby decreasing surface adsorption of the oil to the surface. Another interesting observation is the extent of wettability alteration caused by each oil, presented in the images also in Figure 5 for crude oils A, C, and F. Figure 5 shows how strongly the RF is dependent on the oil type even for the exact same procedure in accurately controlled settings. Therefore, the results from one oil cannot be projected to others.

3.3. Pore-Volumes Injected. Pore-volumes injected is defined as the normalized injected fluid by the volume of the network. One of the variables in an EOR test is the amount of injected fluid. As the flood gets injected into the network, the oil gets extracted, and the RF increases rapidly until it gets to breakthrough. Then, the recovery plateaus and almost only water is produced. In the case of stable displacements (e.g., crude oil F in Figure 4), the flood moves oil with an almost straight frontline that steadily moves toward the outlet. No more change is visible after the flood reaches the end of the network area. In unstable displacements (e.g., crude oils C and A), viscous fingering happens, meaning the flood can get divided into different branches going at different random directions.

https://dx.doi.org/10.1021/acsomega.0c02005
ACS Omega 2020, 5, 17521−17530

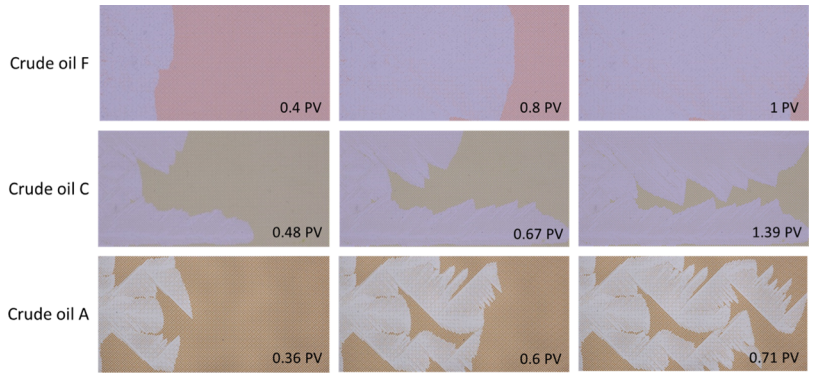

Figure 4. Course of displacement of crude oils F, C, and A by HS-Na at 0.5 μL/min. Pore volumes injected for each image is displaced in the lower right corner of it.

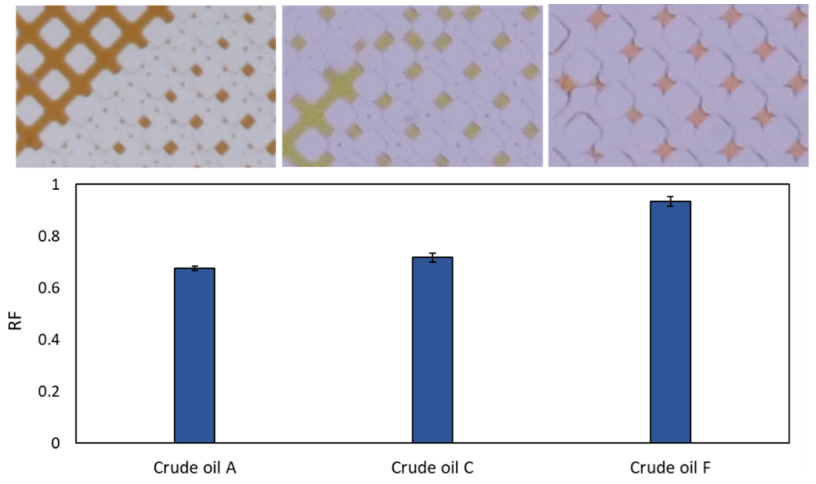

Figure 5. RF for different types of crude oil displaced by HS-Na at 0.5 μL/min. The images above each column are snapshots of the oil and brine in the channels after the flooding is done.

One of the two possibilities can then be expected: single or multiple breakthroughs. Single breakthrough is the more common occurrence in this study, where the oil content does not change after the first stream of flood reaches the outlet. From this point on, the network will only produce water. However, in some cases, after the first breakthrough, the rest of the streams keep moving in the direction of the outlet while displacing more oil. Multiple breakthroughs are also reflected in the pressure recordings. A typical graph for evolution of the RF from the moment the flood reaches the network to the plateau through time is presented in Figure 6. It should be noted that the flood volume required to reach the network is not included in this graph. The point where the slope of the graph suddenly changes (at 2.5 μL) indicates the breakthrough. Shortly after that, the recovery remains constant at 0.65. The straight line through (0,0) is how the recovery would have happened if there were no hindrances or interactions between the three constituents of the process. Depending on the test conditions, it can take shorter or longer to reach a stable residual oil saturation. However, by the time 10 μL of the flood is injected, the remaining oil saturation is stable for all the tests. Therefore, 10 μL of flood volume, equal to 4.8 pore volume, is selected as the flood volume for all tests in this study, including secondary and tertiary stages of EOR tests.

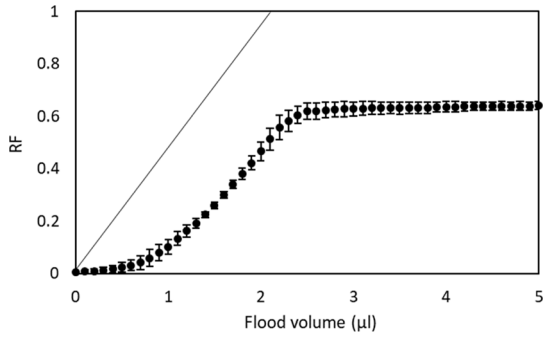

Figure 6. Change of RF with time/flood volume starting from the time the flood reaches the network. Test: crude oil A displaced by LS-NaCa. The straight line through (0,0) represents recovery without hindrance or interactions.

3.4. Flow Rate. Another variable influencing an EOR test is the flood flow rate. To investigate the effect of the injection rate, crude oil A is displaced by HS-Na at different flow rates of 0.03, 0.5, 5, and 50 μL/min. The lowest flow rate corresponds with an injection rate of ca. 1 ft/day. The test results are presented in Table 3. The capillary number grows one order of magnitude with each increasing flow rate. At higher rates (5 and 50 μL/min), the flood runs through the whole area of the network (Figure 7). This is another pattern for unstable displacement observed in this study. It shows almost complete invasion of the chip area by the flood. The water phase spreads out in the porous network but also leaves a lot of oil behind in the channels. Besides, the water path is dynamic and keeps changing with the flow. However, more water running through different areas of

https://dx.doi.org/10.1021/acsomega.0c02005
ACS Omega 2020, 5, 17521−17530

Table 3. Effect of the Flow Rate on Oil Recovery[a]

injection rate (μL/min)	0.03	0.5	5	50
RF	0.686 ± 0.049	0.677 ± 0.008	0.541 ± 0.043	0.562 ± 0.011
time to complete 10 μL of flood	333 min	20 min	2 min	12 s
linear velocity (cm/min)	0.02	0.5	5	50

[a]Test: crude oil A displaced by HS-Na.

Figure 7. Crude oil A displaced by HS-Na at 5 μL/min at 5, 15, and 25 s (breakthrough).

the chip does not necessarily mean complete sweep or stable displacement. In the extreme cases of this type of viscous fingering, water and oil get mixed and emulsification happens. Then, oil-in-water droplets fill the outlet end of the chips. This happens for crude oil A when it is flooded with HS-Na at the highest flow rate (50 μL/min). Most importantly, at higher flow rates, the residence time is likely not enough for the interfacial phenomena between the constituents and what we observe is just one fluid physically pushing another fluid out. Furthermore, it is not feasible in the reservoirs because of excessive pressure buildup and risk of fracturing. For lower flow rates, 0.5 and 0.03 μL/min, the recovery is comparable. However, at an ultralow flow rate of 0.03 μL/min, it takes more than 5 h to pump 10 μL of the fluid, while the experiment lasts only 20 min for 0.5 μL/min. Therefore, 0.5 μL/min is chosen as the standard flow rate for the rest of the tests in this study.

3.5. Initial Brine Saturation. Reservoir rock pores were initially saturated with formation brine before oil invaded the rocks; hence, there is the irreducible water in oil rock pores. To simulate such a situation in the micromodels, initial brine saturation before injecting the crude oil can be performed. Adding this step changes the wettability conditions of the chip surface, although the crude oil and flood do not change. To further investigate such effects, three experiments were conducted: one with HS-Na, one with HS-NaCa, and one without any initial brine saturation. The micromodels were then saturated with crude oil A and subsequently flooded by HS-Na. Figure 8 reveals the results, showing the strong influence of initial brine saturation on the oil recovery. The rate at which the oil is injected into the network can also impact the outcome as it affects the irreducible water saturation. In these tests, the chips are saturated with oil at 0.5 μL/min after the brine saturation.

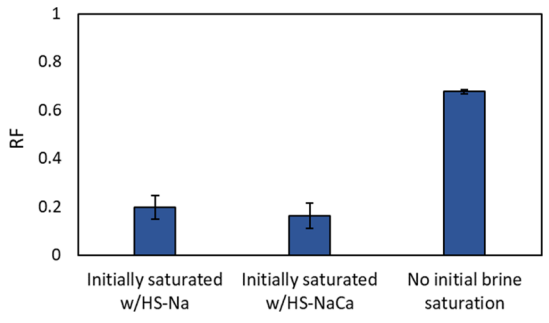

Figure 8. Effect of initial brine saturation. The two test chips on the left are initially saturated with HS-Na and HS-NaCa before the oil saturation step with crude oil A. The oil was then displaced by HS-Na.

Figure 9 shows the difference that the initial brine saturation makes at pore scale. According to the data, there is a dramatic

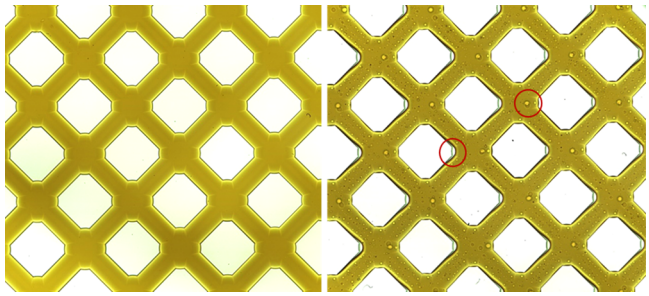

Figure 9. Uniform network area: saturated with crude oil A (left) and initially saturated with brine (HS-Na) and then crude oil A (right). Thin aqueous films and droplets are visible in the right picture.

difference between the RF for tests involving initial brine saturation and the one without. The RF is higher by 48−51% when there is no initial brine saturation. It also changes slightly with the composition of the initial saturating brine, increasing the recovery by 3.5% when there are just monovalent ions present in the brine. The interaction between the oil and the surface without the presence of a brine includes polar interactions or H-bonds, whereas in the presence of brine, the interactions can be acid−base, coulombic, and/or divalent cation bridging. The latter group of interactions are stronger and, therefore, cause a higher affinity between the oil and the chip surface, which in turn results in lower recovery. Also, as soon as the flood was introduced to the network, the water entities connected and created a preferred narrow path which reached breakthrough very fast and left most of the oil in the chip unexposed to the flood. These narrow water paths for all the tests were on the two sides of the chip along the flow direction. In micromodels initially saturated with HS-NaCa, divalent ions bind negatively charged acidic group oil components to the negatively charged surface.[4,38] Because of the stronger bond in the presence of divalent ions, we observed a slightly lower recovery.

3.6. Aging. Allowing the oil to age in the micromodel provides the opportunity for the interfacially active components of oil to adsorb on the intrinsically hydrophilic glass surface. This would make the surface more hydrophobic and could impact the oil recovery results. Including aging in the test better simulates the actual reservoir conditions. This is also often performed in the core flooding tests, where it can take days or weeks.[39,40] Figure 10 presents the results for different aging times. Based on

https://dx.doi.org/10.1021/acsomega.0c02005
ACS Omega 2020, 5, 17521−17530

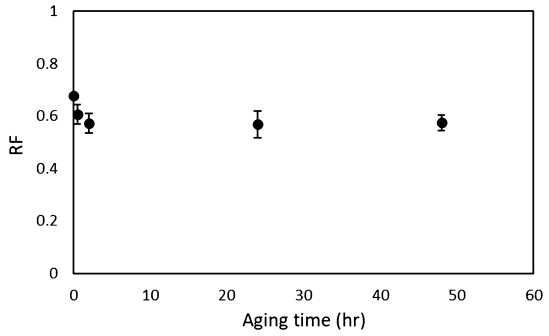

Figure 10. Effect of aging on oil recovery. Crude oil A was aged for different periods of time ranging from 5 min to 48 h and then displaced by HS-Na.

the figure, aging decreases oil recovery by a rather small margin in the first 2 h, and after that point, it reaches a plateau. These results suggest that a 2 h adsorption time after saturating the micromodel with crude oil is a reasonable choice for the microfluidic flooding experiments.

3.7. Brine Concentration. It is suggested in the literature that the LS brine/diluting connate water improves oil recovery by inducing rock wettability change from oil-wet to water-wet and oil desorption.[41,42] It is a favorable method because it does the same changes without the negative environmental impact or the use of expensive chemicals. To investigate the effect of low-salinity flooding, two pairs of tests were designed with crude oils A and C. Each oil was flooded with both LS brine and HS brine. Figure 11 shows the comparison between the results, revealing

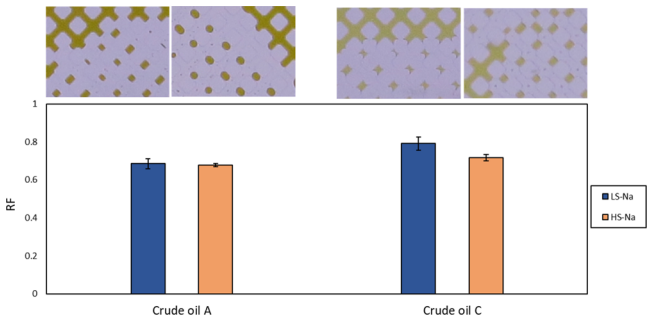

Figure 11. Effect of flood salinity on RF for crude oils A and C.

that the recovery is more effective with LS brine by a small percentage. This applies to both crude oils. LS brine recovers 0.8% more of crude oil A and 7.3% more of crude oil C, compared to the HS brine. Polar components of crude oil adsorb onto the water−oil interface. Thicker Debye length and smaller hindrance of counter ions help with better recovery of oil in LS water flooding.[43] The brine concentration also affects the IFT between the oil and water phase that can also play a role in the recovery. The IFT between crude oil A and high and LS brine is 13.1 and 18.7 mN/m, respectively. Those numbers for crude oil C are 15.5 and 20.1 mM/m, respectively. Moreover, the change in wettability is also visible on the images for each pair of tests.

3.8. Brine Composition/Presence of Divalent Ions. Although the use of only monovalent ions can simplify the experiments, in reality, brines contain different components including divalent ions. To study the effect of divalent ions in the flood, two pairs of tests with different brine compositions were conducted. Crude oil A was flooded by high and LS brine containing either only sodium chloride or both sodium and calcium chlorides. In order to only see the effect of divalent ions, the ionic strength of the two pairs of low and HS brines was kept constant at 0.02 and 0.6 M, respectively. Based on the results shown in Figure 12, the presence of divalent ions (calcium) in

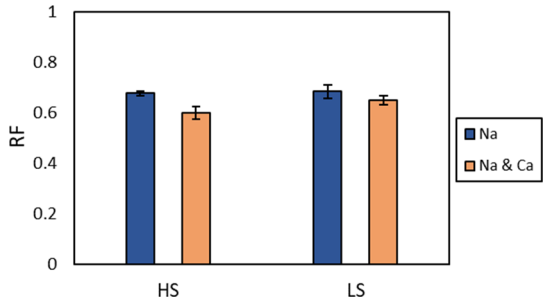

Figure 12. RF for crude oil A displaced by high and LS brine, each with and without calcium ions.

the flood has a negative impact on oil recovery. This finding is independent of the brine concentration. Calcium ions help bridge the negatively charged surface of the wall to the negatively charged components of crude oil and, therefore, create stronger adsorption of crude oil on the surface that better resists the flood and recovery. The presence of calcium can also affect the wettability of the surface, making it more hydrophobic.[42] A similar situation and mechanism was also seen in the initial brine saturation case. Adding divalent ions to the HS water reduced the recovery of crude oil A by 7.8% compared to 3.5% for the LS flood.

3.9. Network Type. Rock network chips have a more complex pore structure and give a more realistic representation of oil displacement in reservoirs. One of the most common scenarios of oil-trapping in water-wet reservoirs is immobilization of the oil drops in narrow pore throats and dead-end pores by capillary forces. To investigate the difference, the same recovery test was conducted with both uniform and rock networks. According to the results (Table 4), the use of the rock

Table 4. Effect of Network Design on RF[a]

	Uniform network	Rock network
Average RF	0.677 ± 0.008	0.48 ± 0.041
Picture at breakthrough		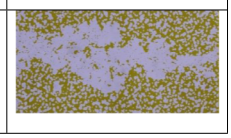

[a]Test: crude oil A displaced by HS-Na

network instead of the uniform network results in lower oil recovery, as anticipated. It was also expected to record a higher pressure for a rock network than a uniform network because of the irregular morphology of the pores and, more importantly, the dead-end pores and narrow throats. This was also confirmed by the maximum recorded pressures of 0.24 and 0.56 bar for uniform and rock networks, respectively. As also visible in the picture, viscous fingering seems to be inevitable in the rock network.

3.10. EOR Tests. The combination of the experimental results presented in the previous sections helped develop a procedure that would be an imitation of the processes happening in the reservoirs. Initial brine saturation and aging are taken into

https://dx.doi.org/10.1021/acsomega.0c02005
ACS Omega 2020, 5, 17521−17530

account, brines with divalent ions are used as aquifer water and floods, HS brine is used during the initial brine saturation and IOR stage as a better representative of seawater, and flood volumes are limited to 10 μL (less than 5 pore volumes), where the saturation has already reached the steady state.

The stages of an EOR test developed based on the previously mentioned test results are as follows:

- Fill the uniform network chip with the HS brine (HS-NaCa).
- Age for 30 min (at ambient conditions).
- Saturate the chip with the oil (crude oil A).
- Age for 2 h (at ambient conditions).
- IOR: flood the chip with 10 μL of HS brine (HS-NaCa) at 0.5 μL/min.
- EOR: flood the chip with 10 μL of LS brine (LS-NaCa) at 0.5 μL/min.

Experiments were conducted following the aforementioned procedure. Figure 13 shows the compiled time-lapse images of

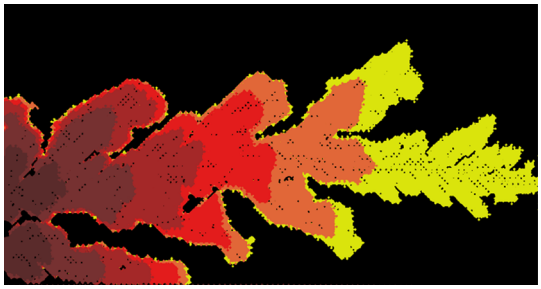

Figure 13. Time-lapse image of the IOR flood through a chip. The early stage is represented by burgundy color and breakthrough by yellow. The voids of the chip (grains) are colored with the same color as the surrounding channels. The interval of the images is 0.19 pore volume of the HS-Na (48 s). Test: initially brine (HS-NaCa) saturated chip, filled with crude oil A and displaced by HS-NaCa.

the HS brine progressing through the chip at the IOR stage. The oil recovers at a fast rate once the flood reaches the network. It usually takes about one pore volume of the HS brine before it gets to the network area. The recovery almost stops shortly after the breakthrough, which usually happens at about two pore volumes.

After injecting about two pore volumes of the HS brine through the micromodel, the remaining oil content of the network does not change, meaning that no more oil would have been extracted had we continued the injection of the same HS brine. After the injection of the HS brine is done, the LS brine is introduced to the network as the tertiary stage of recovery. During the EOR flood, the saturation changes at a very slow pace but manages to recover additional oil. The results for the three separate EOR tests are presented in Figure 14. Note that the graph has a collapsed y-axis and is capped at 0.7, in order for the smaller features to be clearly visible. Because of the higher complications of this test and numerous steps that it involves, a bigger standard deviation is observed. On average, the tests showed 54.4% of total oil recovery from both high and LS floodings, from which an average of 1% was contributed by the tertiary recovery. For the settings of this study, LS water flooding showed to be recovering some small but valuable amount of extra oil.

To investigate the effect of adding the tertiary stage without the complications of initial brine saturation, another experiment

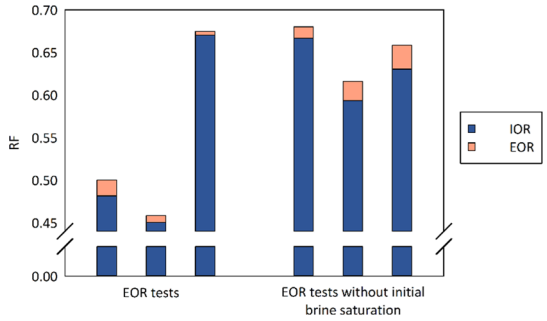

Figure 14. Total RF for crude oil A through secondary and tertiary stages of recovery by HS-NaCa and LS-NaCa brines, respectively. The test also involves initial brine saturation by HS-NaCa for the cluster of columns on the left labeled as EOR tests.

was performed to include just the secondary and tertiary stages of recovery. Figure 14 presents the fraction of oil recovered specifically marking the contribution of IOR and EOR. On average, 63% of the oil was recovered with the HS brine, which is about 10% higher than the case with initial brine saturation. This effect was also observed in Section 3.5. Another 2.1% of the oil gets extracted with the LS brine. The tests show to be more repeatable with a standard deviation of 0.03 for the IOR RF with one step less in the procedure. Different studies have reported a broad range of RFs from 0.00 to 19.53% for LS flooding following HS flooding.[44] However, numbers from microfluidcs and core flooding cannot be directly compared as further validation/comparison studies must be done.

4. CONCLUSIONS

A procedure for a microfluidic EOR process was developed that includes initial brine saturation, representative flood volume and injection rate, aging, and secondary and tertiary stage oil recoveries. The following observations were made in this study:

- The displacement was stable only for the lightest oil (crude oil F).
- The worst cases of instability happened when chips were initially saturated with brine. In these cases, most of the oil remained in the channels and brine got to the outlet through the narrowest pathways. After the breakthrough, oil was no longer mobilized from the network.
- LS brine showed to recover oil more effectively than the HS brine for both crude oils A and C during the one-step recovery tests.
- The presence of divalent ions in the flood or in the water phase in the network prior to the oil saturation decreased oil recovery. Oil recovery declined with both high and LS brine after the addition of calcium to the flood because of stronger interactions between the solid surface and the crude oil.
- Because crude oils are naturally complex fluids, repeatability was important. The small values of standard deviation demonstrated repeatable and reliable experiments.

Based on the evaluations done in this study as well as the obtained results and their consistent comparison with the literature and previous conventional methods, we can conclude that microfluidics can provide a reliable and viable platform for oil recovery studies. Although micromodels are considered as 2D representation of the rock, they can offer numerous advantages that make them an attractive alternative for fluid–

https://dx.doi.org/10.1021/acsomega.0c02005
ACS Omega 2020, 5, 17521−17530

fluid displacement studies. Microfluidics not only provides a visual gateway into the processes happening in the rock network but also reduces the environmental impact and enables us to run experiments in a very controlled environment. However, there is still the potential for further studies testing other parameters and more extreme conditions with microfluidics to better simulate the actual processes. It would also be useful to conduct validation studies utilizing core flooding and the equivalent test conditions and procedures. This would also help translate different real-life conditions into microfluidics and determine how well-represented different factors such as the silicate material and pore structure are.

AUTHOR INFORMATION

Corresponding Authors

Peichun A. Tsai − *Department of Mechanical Engineering, University of Alberta, Edmonton T6G 1H9, Canada*; Phone: +1 7804925425; Email: peichun.amy.tsai@ualberta.ca

Gisle Øye − *Ugelstad Laboratory, Department of Chemical Engineering, Norwegian University of Science and Technology (NTNU), Trondheim 7491, Norway*; orcid.org/0000-0002-6391-3750; Phone: +47 97567011; Email: gisle.oye@chemeng.ntnu.no

Authors

Marzieh Saadat − *Ugelstad Laboratory, Department of Chemical Engineering, Norwegian University of Science and Technology (NTNU), Trondheim 7491, Norway*; orcid.org/0000-0001-8938-4888

Tsai-Hsing Ho − *Department of Mechanical Engineering, University of Alberta, Edmonton T6G 1H9, Canada*

Marcin Dudek − *Ugelstad Laboratory, Department of Chemical Engineering, Norwegian University of Science and Technology (NTNU), Trondheim 7491, Norway*; orcid.org/0000-0001-6444-7109

Complete contact information is available at: https://pubs.acs.org/10.1021/acsomega.0c02005

Notes

The authors declare no competing financial interest.

ACKNOWLEDGMENTS

This project was funded by VISTA, a research partnership between Equinor and the Norwegian Academy of Science and Letters (project number 6365).

REFERENCES

(1) Norwegian Petroleum Directorate. *Resource Report 2017: Even More to Gain.*

(2) Gerold, C. T.; Krummel, A. T.; Henry, C. S. Microfluidic devices containing thin rock sections for oil recovery studies. *Microfluid. Nanofluid.* **2018**, *22*, 76.

(3) Tang, G. Q.; Morrow, N. R. Salinity, temperature, oil composition, and oil recovery by waterflooding. *SPE Reservoir Eng.* **1997**, *12*, 269−276.

(4) Lager, A.; Webb, K. J.; Black, C. J. J.; Singleton, M.; Sorbie, K. S. Low salinity oil recovery−An experimental investigation. *Petrophysics* **2008**, *49*, 28−35.

(5) McGuire, P. L.; Chatham, J. R.; Paskvan, F. K.; Sommer, D. M.; Carini, F. H. Low Salinity Oil Recovery: An Exciting New EOR Opportunity for Alaska's North Slope. *SPE Western Regional Meeting*; Society of Petroleum Engineers: Irvine, California, 2005; p 15.

(6) Seccombe, J.; Lager, A.; Jerauld, G.; Jhaveri, B.; Buikema, T.; Bassler, S.; Denis, J.; Webb, K.; Cockin, A.; Fueg, E. Demonstration of Low-Salinity EOR at Interwell Scale, Endicott Field, Alaska. *SPE Improved Oil Recovery Symposium*; Society of Petroleum Engineers: Tulsa, Oklahoma, USA, 2010; p 12.

(7) Morrow, N.; Buckley, J. Improved Oil Recovery by Low-Salinity Waterflooding. *J. Pet. Sci. Technol.* **2011**, *63*, 106−112.

(8) Yousef, A. A.; Al-Saleh, S.; Al-Jawfi, M. S. Improved/Enhanced Oil Recovery from Carbonate Reservoirs by Tuning Injection Water Salinity and Ionic Content. *SPE Improved Oil Recovery Symposium*, 2012; Vol. *1*.

(9) Tichelkamp, T.; Teigen, E.; Nourani, M.; Øye, G. Systematic study of the effect of electrolyte composition on interfacial tensions between surfactant solutions and crude oils. *Chem. Eng. Sci.* **2015**, *132*, 244−249.

(10) Katende, A.; Sagala, F. A critical review of low salinity water flooding: Mechanism, laboratory and field application. *J. Mol. Liq.* **2019**, *278*, 627−649.

(11) Song, W.; Kovscek, A. R. Direct visualization of pore-scale fines migration and formation damage during low-salinity waterflooding. *J. Nat. Gas Sci. Eng.* **2016**, *34*, 1276−1283.

(12) Yu, M.; Zeinijahromi, A.; Bedrikovetsky, P.; Genolet, L.; Behr, A.; Kowollik, P.; Hussain, F. Effects of fines migration on oil displacement by low-salinity water. *J. Pet. Sci. Eng.* **2019**, *175*, 665−680.

(13) RezaeiDoust, A.; Puntervold, T.; Austad, T. Chemical Verification of the EOR Mechanism by Using Low Saline/Smart Water in Sandstone. *Energy Fuels* **2011**, *25*, 2151−2162.

(14) Austad, T.; Rezaeidoust, A.; Puntervold, T. Chemical Mechanism of Low Salinity Water Flooding in Sandstone Reservoirs. *SPE Improved Oil Recovery Symposium*; Society of Petroleum Engineers: Tulsa, Oklahoma, USA, 2010; p 17.

(15) Johannessen, A. M.; Spildo, K. Enhanced Oil Recovery (EOR) by Combining Surfactant with Low Salinity Injection. *Energy Fuels* **2013**, *27*, 5738−5749.

(16) Pollen, E. N.; Berg, C. F. Experimental Investigation of Osmosis as a Mechanism for Low-Salinity EOR. *Abu Dhabi International Petroleum Exhibition and Conference*; Society of Petroleum Engineers: Abu Dhabi, UAE, 2018; p 20.

(17) Mahani, H.; Berg, S.; Ilic, D.; Bartels, W.-B.; Joekar-Niasar, V. Kinetics of the Low Salinity Waterflooding Effect Studied in a Model System. *SPE Enhanced Oil Recovery Conference*; Society of Petroleum Engineers: Kuala Lumpur, Malaysia, 2013; p 14.

(18) Sharma, H.; Mohanty, K. K. An experimental and modeling study to investigate brine-rock interactions during low salinity water flooding in carbonates. *J. Pet. Sci. Eng.* **2018**, *165*, 1021−1039.

(19) Ding, H.; Rahman, S. Experimental and theoretical study of wettability alteration during low salinity water flooding-an state of the art review. *Colloids Surf., A* **2017**, *520*, 622−639.

(20) Mohammed, M.; Babadagli, T. Wettability alteration: A comprehensive review of materials/methods and testing the selected ones on heavy-oil containing oil-wet systems. *Adv. Colloid Interface Sci.* **2015**, *220*, 54−77.

(21) Lifton, V. A. Microfluidics: an enabling screening technology for enhanced oil recovery (EOR). *Lab Chip* **2016**, *16*, 1777−1796.

(22) Sinton, D. Energy: the microfluidic frontier. *Lab Chip* **2014**, *14*, 3127−3134.

(23) Gogoi, S.; Gogoi, S. B. Review on microfluidic studies for EOR application. *J. Pet. Explor. Prod. Technol.* **2019**, *9*, 2263−2277.

(24) Chen, Y.-F.; Fang, S.; Wu, D.-S.; Hu, R. Visualizing and quantifying the crossover from capillary fingering to viscous fingering in a rough fracture. *Water Resour. Res.* **2017**, *53*, 7756−7772.

(25) Lenormand, R.; Touboul, E.; Zarcone, C. Numerical-Models and Experiments on Immiscible Displacements in Porous-Media. *J. Fluid Mech.* **1988**, *189*, 165−187.

(26) Zhang, C.; Oostrom, M.; Wietsma, T. W.; Grate, J. W.; Warner, M. G. Influence of Viscous and Capillary Forces on Immiscible Fluid Displacement: Pore-Scale Experimental Study in a Water-Wet Micromodel Demonstrating Viscous and Capillary Fingering. *Energy Fuels* **2011**, *25*, 3493−3505.

(27) Farooq, U.; Asif, N.; Tweheyo, M. T.; Sjöblom, J.; Øye, G. Effect of Low-Saline Aqueous Solutions and pH on the Desorption of Crude Oil Fractions from Silica Surfaces. *Energy Fuels* **2011**, *25*, 2058−2064.
(28) Nourani, M.; Tichelkamp, T.; Gaweł, B.; Øye, G. Desorption of crude oil components from silica and aluminosilicate surfaces upon exposure to aqueous low salinity and surfactant solutions. *Fuel* **2016**, *180*, 1−8.
(29) Xu, K.; Zhu, P.; Huh, C.; Balhoff, M. T. Microfluidic Investigation of Nanoparticles' Role in Mobilizing Trapped Oil Droplets in Porous Media. *Langmuir* **2015**, *31*, 13673−13679.
(30) Buchgraber, M.; Al-Dossary, M.; Ross, C. M.; Kovscek, A. R. Creation of a dual-porosity micromodel for pore-level visualization of multiphase flow. *J. Pet. Sci. Eng.* **2012**, *86*−*87*, 27−38.
(31) Wegner, J.; Ganzer, L. Rock-on-a-Chip Devices for High p, T Conditions and Wettability Control for the Screening of EOR Chemicals. *SPE Europec Featured at 79th EAGE Conference and Exhibition*; Society of Petroleum Engineers: Paris, France, 2017; p 14.
(32) Liu, Y.; Kaszuba, J.; Oakey, J. Microfluidic investigations of crude oil-brine interface elasticity modifications via brine chemistry to enhance oil recovery. *Fuel* **2019**, *239*, 338−346.
(33) Kim, J.; Willmott, E.; Quintero, L. Microfluidics Technology for Visualizing Surfactant Performance in Enhanced Oil Recovery. *IOR 2019—20th European Symposium on Improved Oil Recovery*, 2019; Vol. *2019* (1), pp 1−18.
(34) Dudek, M.; Bertheussen, A.; Dumaire, T.; Øye, G. Microfluidic tools for studying coalescence of crude oil droplets in produced water. *Chem. Eng. Sci.* **2018**, *191*, 448−458.
(35) Tichelkamp, T.; Vu, Y.; Nourani, M.; Øye, G. Interfacial Tension between Low Salinity Solutions of Sulfonate Surfactants and Crude and Model Oils. *Energy Fuels* **2014**, *28*, 2408−2414.
(36) Jakobsen, T. D.; Simon, S.; Heggset, E. B.; Syverud, K.; Paso, K. Interactions between Surfactants and Cellulose Nanofibrils for Enhanced Oil Recovery. *Ind. Eng. Chem. Res.* **2018**, *57*, 15749−15758.
(37) Khanamiri, H. H.; Enge, I. B.; Nourani, M.; Stensen, J. Å.; Torsaeter, O.; Hadia, N. EOR by Low Salinity Water and Surfactant at Low Concentration: Impact of Injection and in Situ Brine Composition. *Energy Fuels* **2016**, *30*, 2705−2713.
(38) Gao, J.; Nair, S.; Duits, M. H. G.; Otto, C.; Mugele, F. Combined microfluidics-confocal Raman microscopy platform for studying enhanced oil recovery mechanisms. *J. Raman Spectrosc.* **2019**, *50*, 996−1007.
(39) Alshakhs, M. J.; Kovscek, A. R. Understanding the role of brine ionic composition on oil recovery by assessment of wettability from colloidal forces. *Adv. Colloid Interface Sci.* **2016**, *233*, 126−138.
(40) Alvarado, V.; Garcia-Olvera, G.; Hoyer, P.; Lehmann, T. E. Impact of Polar Components on Crude Oil-Water interfacial Film Formation: A Mechanisms for Low-Salinity Waterflooding. *SPE Annual Technical Conference and Exhibition*; Society of Petroleum Engineers: Amsterdam, The Netherlands, 2014; p 15.
(41) Ding, H.; Rahman, S. Experimental and theoretical study of wettability alteration during low salinity water flooding-an state of the art review. *Colloids Surf., A* **2017**, *520*, 622−639.
(42) Yang, J.; Dong, Z.; Yang, Z.; Lin, M. Wettability Alteration by Salinity and Calcium Bridge in a Crude Oil/Brine/Rock System. *J. Pet. Sci. Technol.* **2015**, *33*, 1660−1666.
(43) Chávez-Miyauchi, T. E.; Firoozabadi, A.; Fuller, G. G. Nonmonotonic Elasticity of the Crude Oil-Brine Interface in Relation to Improved Oil Recovery. *Langmuir* **2016**, *32*, 2192−2198.
(44) Chávez-Miyauch, T. E.; Lu, Y.; Firoozabadi, A. Low salinity water injection in Berea sandstone: Effect of wettability, interface elasticity, and acid and base functionalities. *Fuel* **2020**, *263*, 116572.

https://dx.doi.org/10.1021/acsomega.0c02005
ACS Omega 2020, 5, 17521−17530